Mohammad Alauhdin 132307273

DRAFT Templated

sci comm 1

Document Details

Submission ID
trn:oid:::3618:118902798

Submission Date
Oct 29, 2025, 5:58 AM GMT+7

Download Date
Oct 29, 2025, 6:15 AM GMT+7

File Name
DRAFT Templated.docx

File Size
856.7 KB

11 Pages

7,217 Words

41,373 Characters

13% Overall Similarity

The combined total of all matches, including overlapping sources, for each database.

Filtered from the Report

- Bibliography
- Small Matches (less than 10 words)

Exclusions

- 1 Excluded Source
- 8 Excluded Matches

Match Groups

56 Not Cited or Quoted 11%
Matches with neither in-text citation nor quotation marks

10 Missing Quotations 2%
Matches that are still very similar to source material

0 Missing Citation 0%
Matches that have quotation marks, but no in-text citation

0 Cited and Quoted 0%
Matches with in-text citation present, but no quotation marks

Top Sources

8% Internet sources
8% Publications
7% Submitted works (Student Papers)

Integrity Flags

0 Integrity Flags for Review

Our system's algorithms look deeply at a document for any inconsistencies that would set it apart from a normal submission. If we notice something strange, we flag it for you to review.

A Flag is not necessarily an indicator of a problem. However, we'd recommend you focus your attention there for further review.

Match Groups

- **56** Not Cited or Quoted 11%
  Matches with neither in-text citation nor quotation marks
- **10** Missing Quotations 2%
  Matches that are still very similar to source material
- **0** Missing Citation 0%
  Matches that have quotation marks, but no in-text citation
- **0** Cited and Quoted 0%
  Matches with in-text citation present, but no quotation marks

Top Sources

8% Internet sources
8% Publications
7% Submitted works (Student Papers)

Top Sources

The sources with the highest number of matches within the submission. Overlapping sources will not be displayed.

1	Internet	
www.mdpi.com		1%
2	Internet	
link.springer.com		<1%
3	Student papers	
Ho Chi Minh University of Technology and Education on 2025-09-21		<1%
4	Publication	
Sofia A. Khromova, Andrey A. Smirnov, Olga A. Bulavchenko, Andrey A. Saraev et ...		<1%
5	Publication	
M Al-Muttaqii, F Kurniawansyah, D H Prajitno, A Roesyadi. "Hydrocarbon Biofuel ...		<1%
6	Internet	
journal.bcrec.id		<1%
7	Student papers	
Tshwane University of Technology on 2022-05-01		<1%
8	Student papers	
Universitas Katolik Indonesia Atma Jaya on 2025-07-07		<1%
9	Publication	
Wenhe Wang, Changsen Zhang, Guanghui Chen, Ruiqin Zhang. "Influence of CeO...		<1%
10	Student papers	
Universitas Trunojoyo on 2025-10-10		<1%

11	Student papers	
University of Sheffield on 2024-10-24		<1%
12	Publication	
Wanli Ma, Chenghui Wang, Zhiqiang Chen, Shuai Yan, Shan Cao, Xianhua Wang, Y...		<1%
13	Publication	
Soheil Valizadeh, Seong-Ho Jang, Gwang Hoon Rhee, Jechan Lee et al. "Biohydrog...		<1%
14	Internet	
www.preprints.org		<1%
15	Internet	
www.iiste.org		<1%
16	Student papers	
Higher Education Commission Pakistan on 2018-05-09		<1%
17	Student papers	
University of Aberdeen on 2021-05-02		<1%
18	Publication	
Zhiwei Shi, Lijun Jin, Yang Zhou, Heng Li, Yang Li, Haoquan Hu. "In-situ analysis of...		<1%
19	Publication	
Afrida Nur Aini, Muhammad Al-Muttaqii, Achmad Roesyadi, Firman Kurniawansy...		<1%
20	Publication	
Bin Li, Ruixia Liu, Hongjie Gao, Ruijie Tan, Ping Zeng, Yonghui Song. "Spatial distri...		<1%
21	Student papers	
The University of Manchester on 2015-09-17		<1%
22	Student papers	
University of Witwatersrand on 2025-01-21		<1%
23	Internet	
pure.tue.nl		<1%
24	Internet	
scholar.archive.org		<1%

25 Publication
R. Miandad, M.A. Barakat, Asad S. Aburiazaiza, M. Rehan, A.S. Nizami. "Catalytic p... <1%

26 Publication
Raditya Hanandika Agharadatu, Karna Wijaya, Prastyo, Wangsa, Latifah Hauli, W... <1%

27 Publication
Yan, Qiangu, Yongwu Lu, Caixia Wan, Jun Han, Jose Rodriguez, Jing-jing Yin, and F... <1%

28 Internet
coek.info <1%

29 Internet
www.jesc.ac.cn <1%

30 Publication
Huynh, Thuan Minh, Udo Armbruster, Marga-Martina Pohl, Matthias Schneider, J... <1%

31 Student papers
Institut Pertanian Bogor on 2023-03-30 <1%

32 Publication
Latifah Hauli, Karna Wijaya, Akhmad Syoufian. "Hydrocracking of LDPE Plastic Wa... <1%

33 Student papers
Leyton Sixth Form College, London on 2020-03-30 <1%

34 Publication
Prem Kumar Seelam, Harisankar Sreenivasan, Satu Ojala, Satu Pitkäaho et al. "M... <1%

35 Publication
Syamsiro, Mochamad, Wu Hu, Shuta Komoto, Shuo Cheng, Putri Noviasri, Pandji ... <1%

36 Student papers
Universiti Teknologi Malaysia on 2011-02-14 <1%

37 Student papers
Universiti Teknologi Malaysia on 2016-09-19 <1%

38 Publication
Yu Li, Changsen Zhang, Yonggang Liu, Songshan Tang, Guanghui Chen, Ruiqin Zh... <1%

39 Internet

www.derpharmachemica.com <1%

40 Publication

"Proceedings of the 10th International Conference and Exhibition on Sustainable ... <1%

41 Publication

Birce Pekmezci Karaman, Nuray Oktar. "Tungstophosphoric acid incorporated hie... <1%

42 Publication

Haswin Kaur Gurdeep Singh, Suzana Yusup, Armando T. Quitain, Bawadi Abdullah... <1%

43 Student papers

Universitas Muhammadiyah Surakarta on 2025-07-08 <1%

44 Student papers

Universitas Sebelas Maret on 2022-08-23 <1%

45 Internet

ejurnal.itats.ac.id <1%

46 Internet

journal.ijresm.com <1%

47 Internet

jurnal.ar-raniry.ac.id <1%

48 Internet

perpustakaan.poltekkes-malang.ac.id <1%

49 Internet

worldwidescience.org <1%

50 Internet

www.research.manchester.ac.uk <1%

Int. J. Renew. Energy Dev. 20xx, x (xx), xx-xx

| xx

Contents list available at CBIORE journal website

International Journal of Renewable Energy Development

Journal homepage: https://ijred.cbiore.id

Review/Research Article

The Effect of Temperature during the Hydrocracking of Low-Density Polyethylene Using a Ni-Cu/HZSM-5 Catalyst

Suhailah Salma Maulida[a], Sri Kadarwati[a*], Adid Adep Dwiatmoko[b], Egi Agustian[c]

[a]*Chemistry Study Program, Universitas Negeri Semarang, Sekaran Campus Bld. D6, Gunungpati, Semarang City, Central Java, Indonesia 50229.*

[b] *Research Center for Catalysis, National Research and Innovation Agency, KST BJ Habibie Build. 452, Tangerang Selatan, Indonesia 15341.*

[c]*Research Center for Molecular Chemistry, National Research and Innovation Agency (BRIN), KST BJ Habibie Build. 452, Tangerang Selatan, Indonesia 15341.*

List of ORCID of each author
ORCID author 1: https://orcid.org/0000-000-xxx-xxx
ORCID author 2: https://orcid.org/0000-0002-4530-1996
ORCID author 3: https://orcid.org/0000-0002-5428-2731
ORCID author 4: https://orcid.org/0000-0003-0944-839X

Abstract. LDPE plastics contributed 20-30% of the plastics use. Due to its non-biodegradable properties, plastic waste management is crucial. In the other hand, the LDPE plastics provide potential and benefits in the exploration of energy resources; they could be converted to liquid fuels through a catalytic hydrocracking. This study focuses on the effect of temperatures during the hydrocracking of LDPE using a Ni-Cu/HZSM-5 catalyst. The Ni-Cu/HZSM-5 catalyst was synthesized using the wet impregnation method assisted by ultrasonic irradiation. The characteristics of the catalyst were evaluated prior to its use during the hydrocracking of LDPE. This study showed that the impregnation of Ni and Cu at HZSM-5 surface did not significantly affect the crystallinity of HZSM-5. Even though the peaks of Ni and Cu in the diffraction pattern were not clearly observed, their presence at HZSM-5 surface was well confirmed by the XRF spectrum. In addition, the hierarchical structure of HZSM-5 was also confirmed by the appearance of microporosity together with the type-IV hysteresis loop on the nitrogen adsorption-desorption isotherm. A considerable decrease (~25%) of the catalyst acidity was observed after the impregnation of Ni and Cu at HZSM-5 surface. The Ni-Cu/HZSM-5 catalyst showed a good activity during the hydrocracking of LDPE at temperatures of 275–400 °C, resulting in liquid, solid, and gas products. The yields of the liquid product increased by increasing the hydrocracking temperatures. It was observed that by increasing the hydrocracking temperatures, the yield of the kerosene and diesel fractions decreased, while the yield of the gasoline fraction increased, as supported by the density and calorific value that was close to the commercial gasoline. A further temperature increase would lead to more products with lighter fractions, reducing the yield of gasoline. This was also supported by the presence of alkenes, ketones, and esters formed after the catalytic hydrocracking as shown by the FTIR spectra of the liquid products.

Keywords: LDPE plastics, catalytic hydrocracking, Ni-Cu/HZSM-5 catalyst.

Received: xxx; Revised: xxxx; Accepted: xxx; Available online: xxx

1. Introduction

The growing population and rapid industrial development have led to increased fuel consumption, especially oil-based fuels (Wardhana *et al.* 2022). However, the domestic oil production has decreased over years due to the limited and dwindling oil supplies. In Indonesia, the amount of oil reserves has declined in the last 10 years (National Energy Council 2023), promoting the alternative measures to overcome the energy gap.

On the other hand, plastics have become the dominant material used in every sector of the economy, causing the amount of plastic waste to increase by 96% from the Covid-19 pandemic (Marbun *et al.* 2021). Low density polyethylene (LDPE) is one of the most widely used types of polyethylene plastic in the world. Approximately 20-30% of plastic waste consisted of LDPE plastic (Li *et al.* 2022). LDPE plastic is widely used as plastic bags and as packaging for food or beverages, as well as packaging for online shopping products. It is low cost, has easy production process, flexibility, and recyclability (Hariadi *et al.* 2021). This plastic is lightweight and has a low density, ranging from 0.91 to 0.94 g/mL, due to the presence of some branches in its molecular chain (Genet *et al.* 2021). LDPE plastic waste has the potential to be converted into liquid fuels, reducing the accumulation of plastic waste and providing a new source of fuel oil using plastic as a raw material (Surono 2013).

Several methods can be used to convert plastics into liquid fuel, such as thermal cracking, catalytic cracking, and hydrocracking. Hydrocracking is one of the most commonly used methods for converting plastic waste into high-quality liquid fuel. This method is more advantageous than thermal cracking and catalytic cracking because it produces highly

* Corresponding author
Email: srika@mail.unnes.ac.id (Sri Kadarwati)

https://doi.org/10.61435/ijred.x.x.xxx-xxx
ISSN: 2252-4940/© 20xx.The Author(s). Published by CBIORE

saturated liquid products that can be used directly, without further processing, as transportation fuel or petroleum fuel required for energy production (Munir *et al.* 2018). Hydrocracking involves a break-down of long-chain hydrocarbon molecules into short-chain hydrocarbon molecules at high pressure using hydrogen and a catalyst (Al-Salem *et al.* 2017).

Catalysts play an important role during the hydrocracking. The catalyst with cracking and hydrogenation-dehydrogenation activities is preferable, such as transition metals, e.g., Cu, Ni, Mo, Co, Pt, Rh, Ru, and Pd. Ni metal has been widely used as a catalyst in the petroleum industry due to its sufficient activity and selectivity during the hydrocracking (Savitri *et al.* 2016). Ni is able to activate hydrogen bonds by adsorbing hydrogen gas at the catalyst surface, facilitating the reaction. The larger the catalyst surface area, the more hydrogen gas absorbed and the more contact occurs between reacting substances, increasing the reaction rate (Lao *et al.* 2025). A promoter metal is often necessary for a metal active catalyst. Copper (Cu) is a good-activity and -selectivity and low-cost promoter for a catalyst system (Khromova *et al.* 2014). The addition of Cu to Ni-based catalysts would result in changes in the catalytic activity and selectivity compared to a monometallic Ni catalyst. Cu could prevent the formation of coke and sintering of active phase particles (Khromova *et al.* 2014). Furthermore, the presence of a support in the catalyst system would further enhance the catalytic activity of the Ni-Cu catalysts. H-Zeolite Socony Mobile-5 (HZSM-5) is one of the most commonly used zeolites as a catalyst in hydrocracking processes, due to its high thermal stability, strong acidity, ability to concentrate reactants within the pores, and well-developed mesopores, which lead to higher activity and stability (Valizadeh *et al.* 2022). HZSM-5 is a type of zeolite with an MFI-type framework and has a high molar ratio of SiO_2/Al_2O_3, ranging from 10 to 100.

The study on the synthesis and application of the Ni-Cu/HZSM-5 catalyst prepared through impregnation-ultrasonic-assisted method during the hydrocracking of LDPE plastic waste is scarce. Therefore, this study focuses on the catalytic hydrocracking of LDPE plastics using the Ni-Cu/HZSM-5 catalyst at temperatures of 275–400 °C. The properties of the Ni-Cu/HZSM-5 catalyst were evaluated by means of several analytical techniques. Furthermore, the effect of reaction temperature on the activity of the Ni-Cu/HZSM-5 catalyst was investigated during the hydrocracking of LDPE plastic. Hydrocracking temperature is crucial parameter as it could reveal the behavior of reactant molecules, products, and catalysts during the reaction (Sinaga *et al.* 2014).

2. Materials and Methods

2.1 The Ni-Cu/HZSM-5 catalyst preparation and characterization

The Ni-Cu/HZSM-5 catalyst was synthesized using the wet impregnation method with ultrasonic irradiation using $Ni(NO_3)_2.6H_2O$ and $Cu(NO_3)_2.3H_2O$ as precursor, with a Ni:Cu metal ratio of 1:1 and a total metal loading of 5wt%. An alternate loading of metal precursor was employed; nickel was impregnated first, followed by copper impregnation. Ultrasonic irradiation was applied in both impregnations. Briefly, HZSM-5 support was added into the nickel solution under a magnetic stirring for 3 h. The sample was then placed in a sonication bath at 40 °C for 60 min. The sample was then evaporated until the water evaporated, leaving only the solid residue. The residue was then heated in an oven at 120 °C for 12 h to remove any remaining water. The solid was then calcined for 3 h at 500 °C. The calcined solid was then further impregnated using copper precursor with the same procedure as previously explained. The solid obtained after this step is assigned as the Ni-Cu/HZSM-5 catalyst.

The properties of the Ni-Cu/HZSM-5 catalyst were evaluated by using several analytical techniques. The crystalline properties of the catalyst were evaluated using a Rigaku SmartLab powder X-ray diffractometer with Cu-K_α as the radiation source. The sample was scanned through 2-tetha of 5-90°. The metal composition of the catalyst was measured using a Bruker S2 PUMA X-ray fluorescence spectrometer. The surface morphology of the catalyst was also investigated by using a Jeol–JIB-4610F field emission scanning electron microscope equipped with an energy dispersive X-ray analysis. The surface porosity of the catalyst was measured by using a Quantachrome Nova Station C gas sorption analyzer with nitrogen as the adsorbate gas. The catalyst sample was degassed at 250 °C for 3 h to remove the moisture. The data was then analyzed using a BET-BJH adsorption-desorption isotherm. In addition, the surface acidity of the catalyst was also measure by using an Autochem II Micromeritics NH_3-Temperature Programmed Desorption. The sample was heated at 350 °C for 60 min under inert helium atmosphere. A 5% NH3 in He (v/v) was used as an adsorbate. The NH_3 adsorption was carried out at 100 °C for 30 min. A helium purging was then performed at the same temperature for 30 min. The NH_3 desorption was then carried out at 100–800 °C with a temperature increment of 10 °C/min.

2.2 Catalytic hydrocracking of pyrolyzed LDPE plastic waste

LDPE plastic used in this study was black-colored LDPE plastic used for online shopping packaging. The plastics were cleaned, cut into small squares prior to pyrolysis. The prepared plastic was then placed in a pyrolysis reactor equipped with a furnace, thermocouple, and temperature controller. The pyrolysis reactor was connected to a nitrogen gas inlet. The nitrogen gas served as a carrier gas that also minimized the presence of oxygen or air in the reactor. The pyrolysis of LDPE plastics was carried out at 500 °C with a flow rate of nitrogen of 50 mL/min. The vapor produced from the pyrolysis reactor entered a condenser connected to a chiller, which circulated the cold water (with a temperature of 4 °C) through the condenser. The condensed product was collected using a jar installed at the end of the condensing system. The gas outlet was left open at the end of the system adjacent to the pipe leading to the liquid product jar. The process was stopped once it reached 1 h (starting from when the reactor reached 500 °C).

The condensed product from the pyrolysis of LDPE plastics underwent a catalytic hydrocracking using a batch reactor equipped with a furnace, thermocouple, and temperature controller. The hydrocracking was conducted at various temperatures, ranging from 275 to 400 °C. At each experiment, a 10 g of the pyrolysis product together with 10 wt% of the Ni-Cu/HZSM-5 catalyst was introduced to the reactor vessel. Prior to the hydrocracking, the reactor was flushed with hydrogen several times and pressurised using a 60-bar hydrogen. The reaction was stopped after 2 h. After each experiment, the liquid product was recovered and then analyzed using an Agilent 7890B gas chromatograph equipped with an Agilent 5977A mass selective detector to determine the yield of the fuel fractions.

The yield of each fraction of fuels was calculated by multiplying the relative area percentage of the product compounds by the weight of the liquid products as shown in Equation (1), (2), and (3). Additionally, the specific gravity and calorific value of the hydrocracking liquid products at various temperatures were measured using pycnometer and ultimate analysis, respectively. The chemical functionalities of the liquid

ISSN: 2252-4940/© xxx. The Author(s). Published by CBIORE

product obtained from the catalytic hydrotreatment was evaluated using a Bruker-Tensor II Fourier-Transformed IR spectrophotometer with an Attenuated Total Reflectance (ATR) sampling technique at wavenumbers 4000-500 cm^{-1}.

$$\text{Gasoline yield (\%)} = \frac{\%\ A_{gasoline} \times W_{liquid}}{W_{feedstock}} \times 100\% \quad (1)$$

$$\text{Kerosene yield (\%)} = \frac{\%\ A_{kerosene} \times W_{liquid}}{W_{feedstock}} \times 100\% \quad (2)$$

$$\text{Diesel yield (\%)} = \frac{\%\ A_{diesel} \times W_{liquid}}{W_{feedstock}} \times 100\% \quad (3)$$

3. Results and Discussion

3.1 Catalyst Characterization

The crystal structure of HZSM-5 and the Ni-Cu/HZSM-5 catalyst was investigated using an X-ray diffractometer, as is shown in Fig. 1. There was no significant difference between the diffraction pattern of HZSM-5 and that of the Ni-Cu/HZSM-5 catalyst. The addition of Ni and Cu metals did not change the crystal structure of HZSM-5. However, a decrease in the intensity of diffraction peaks of the Ni-Cu/HZSM-5 catalyst was observed. This might be related to the rearrangement of molecules within the pores of HZSM-5 following the addition of Ni and Cu metals, leading to a reduction of X-ray scattering (Marlinda *et al.* 2017).

The HZSM-5 support showed specific diffraction peaks at 2θ of 7-8° and 23-24° (Tursunov *et al.* 2019). In this study, the XRD results showed diffraction peaks for HZSM-5 at 2θ of 7.83°, 8.73°, 22.97°, 23.17°, 23.79°, and 24.28°. The presence of Ni metal, according to Joint Committee on Powder Diffraction Standards (JCPDS) No. 00-004-0850, was observed at 2θ of 44.5° (111) and 51.84° (200). However, those two peaks could not be clearly observed in the diffraction patterns. This might indicate that Ni was finely dispersed on the catalyst surface or not separated on the pore walls of the sample (Akça *et al.* 2007). While, the presence of Cu metal, according to JCPDS No. 00-003-1018, was observed at 2θ of 43.2°, 50.3°, and 70.0°. Again, there was no significant peaks observed in the diffraction patterns indicating the presence of Cu metal; a small peak or shoulder peak (Fig. 1(b)) appeared at 2θ of 43.25°, which may indicate the presence of a Cu metal peak ((111) crystal plane, indicating the cubic structure) (Zheng *et al.* 2021).

The presence of Ni and Cu metals in the Ni-Cu/HZSM-5 catalyst, which is an indication of successful impregnation, was also be evaluated through characterization using other methods, such as X-ray fluorescence spectroscopy and scanning electron microscopy. The elemental composition in Table 1 shows that the metal components present in the HZSM-5 carrier were Si and Al, with respective weights of 43.00% and 2.90%. This is in accordance with the definition of zeolite, which consists of silica and alumina.

The relative composition of Si and Al in the HZSM-5 support was a bit higher than that in the Ni-Cu/HZSM-5 catalyst due to the addition of Ni and Cu metals. The weight percentage of Si and Al decreased from 43.00% and 2.90% to 39.40% and 2.80%, respectively. The introduction of Ni and Cu into the HZSM-5 structure may cause micro-pore blockage that could hinder the accessibility of Si and Al sites for XRF measurement, which effectively reduced the apparent concentration in the analysis (Nugrahaningtyas *et al.* 2024; Wang *et al.* 2019). The elemental analysis using XRF indicated that Ni and Cu metals were successfully introduced at the HZSM-5 surface, while the diffraction patterns did not say so.

The surface properties of the Ni-Cu/HZSM-5 catalyst were also investigated using a field emission scanning electron microscope (FESEM) equipped with energy dispersive X-ray (EDX) spectroscopy to determine the elemental composition, especially Si, Al, Ni and Cu in both materials. The surface morphology of HZSM-5 and Ni-Cu/HZSM-5 is shown in Fig. 2, while the elemental composition is listed in Table 2. It was observed from Fig. 2(a) that the morphology of HZSM-5 showed a uniform shape as hexagonal crystals. A slight difference in the morphological structures between HZSM-5 and Ni-Cu/HZSM-5 was observed. Small dots and clumps around HZSM-5 assigned as Ni and Cu metals were observed in Fig. 2(b). The addition of Ni and Cu metals to HZSM-5 did not change the crystal structure of HZSM-5. The objects visible surrounding the surface of the HZSM-5 zeolite, shown in an area that is brighter than the surrounding area, were an agglomeration of Cu metal, which can be proven using Energy Dispersive X-ray (EDX) analysis in Table 2 and Fig. 2(c-e).

The results of the EDX analysis show that Ni metal is evenly distributed on the HZSM-5 carrier, as shown in Fig. 2(d). This distribution is indicated by the yellow color, which symbolizes Ni metal scattered throughout the HZSM-5 carrier, with a weight percentage of 2.7%. Fig. 2(e) shows the distribution of Cu metal impregnated on HZSM-5 zeolite. The uneven distribution of Cu metal in this catalyst impregnation can be seen from the high Cu content compared to Ni in Table 2, which was 13.9%. Metal distribution can be influenced by the impregnation technique used to add metal to the catalyst. If the metal precursor solution was uneven or insufficient to fill all pores, there would be unevenness in the distribution of Cu metal. In addition, suboptimal stirring can also cause some areas of the support to not be filled properly with metal, causing variations in metal concentration (Zultiniar *et al.* 2017).

In addition to surface morphology, the surface porosity of HZSM-5 and Ni-Cu/HZSM-5 catalyst was evaluated using adsorption-desorption behavior of liquid nitrogen at the solid surface. By using Brunauer-Emmett-Teller (BET) and Barrett-Joyner-Halenda (BJH) adsorption-desorption isotherms, the surface area, pore diameter, and pore volume of the catalyst were analyzed, as is shown in Table 3. The results of the study in Table 3 show that there was a considerable increase (34.44%) in the surface area of HZSM-5 after impregnation of Ni and Cu metals from 201.699 m^2/g to 271.167 m^2/g. It was likely due to the distribution of the metals at the zeolite surface, causing unevenness, which results in an increase in surface area (Nugrahaningtyas *et al.* 2024). This increase in the surface area would show a good effect on the catalyst activity since a large surface area would have more active phases distributed, thereby increasing catalyst activity. Catalysts with a high surface area allow for more contact between reactant molecules and the catalyst, which can influence the overall catalytic process (Savitri *et al.* 2016).

In addition to the increase in the surface area of the Ni-Cu/HZSM-5 compared to the HZSM-5 support, a considerable increase (32.73%) in the pore volume of the Ni-Cu/HZSM-5 catalyst (from 0.1537 cm^3/g to 0.2040 cm^3/g) was also observed, as is shown in Table 3. The presence of Ni and Cu metals that might enter the pore mouths could slightly expand the pore size, thereby increasing the total pore volume (Nugrahaningtyas *et al.* 2024). However, the increase in the surface area and pore volume was not accompanied by the change in the pore diameter of HZSM-5 after the introduction of Ni and Cu metals. There was no significant increase of this pore diameter of HZSM-5 before and after impregnation with Ni and Cu metals. The pore diameter of HZSM-5 zeolite and Ni-Cu/HZSM-5 catalyst in this study was 1.9119 and 1.9125 nm,

ISSN: 2252-4940/© xxx. The Author(s). Published by CBIORE

respectively, indicating that the catalyst is a microporous material.

The adsorption-desorption isotherm of liquid nitrogen at the HZSM-5 and Ni-Cu-HZSM-5 surface as shown in Fig. 3 showed a similar pattern; a type IV adsorption-desorption isotherm. Type IV isotherms show the characteristic of mesoporous solids, as indicated by the presence of a hysteresis loop at $P/P_0 > 0.4$. The BET-BJH analysis in Table 3 showed that the pore sizes <2 nm in HZSM-5 and Ni-Cu/HZSM-5, indicating microporosity. However, the presence of a type IV hysteresis loop in the adsorption-desorption isotherm indicated mesoporous porosity, which corresponds to pores in the range of 2–50 nm. This difference can be explained by the hierarchical structure of HZSM-5, which had both micro- and mesopores. HZSM-5 can have both micropores and mesopores, resulting in combined features in adsorption analysis. Therefore, the BET and hysteresis loop results were not contradictory but complementary, indicating that the sample has a microporous framework with mesoporous characteristics that likely originate from a hierarchical structure or secondary porosity (Gorzin *et al.* 2018; Karim *et al.* 2024).

The number and strength of surface acidity were a good measure of a catalyst activity. The surface acidity of HZSM-5 and Ni-Cu/HZSM-5 catalysts was analyzed using the ammonia-temperature-programmed desorption (NH_3-TPD) method. The NH_3-TPD analysis was performed to determine the effect of catalyst acidity based on NH_3 gas adsorption. In this study, the results in Table 3 showed that the acidity of HZSM-5 considerably decreased (24.54%) after the addition of Ni and Cu metals from 3.2679 mmol/g to 2.4631 mmol/g. This decrease in acidity may be influenced by the metal impregnation process on the acid sites. The loading of Ni and Cu metals could replace some of the protons responsible for the Bronsted acid sites on HZSM-5, causing a decrease in Bronsted acidity and a change in the balance between Bronsted and Lewis acid sites. This exchange could reduce the total number of acid sites available for NH_3 adsorption, thereby lowering the acidity value measured by NH_3-TPD (Qin *et al.* 2023).

3.1 Hydrocracking of Pyrolyzed LDPE Plastics Using Ni-Cu/HZSM-5 Catalyst

The process of converting LDPE plastic into liquid fuel fractions was carried out in two stages, namely LDPE plastic pyrolysis followed by catalytic hydrocracking of the pyrolysis product using Ni-Cu/HZSM-5 catalyst. Thermal degradation of LDPE plastic in this study produced wax, char, and non-condensable gas. The color of the wax product was brownish-yellow. The wax resulting from the pyrolysis process was then used as the feedstock during the hydrocracking in the presence of Ni-Cu/HZSM-5 catalyst at different temperatures.

The main product of the hydrocracking reaction is a liquid product. Liquid products generally increase with increasing reaction temperature as is shown in Fig. 4. The increase in liquid yield was associated with increased catalyst activity and cracking rate at higher temperatures. High temperatures accelerate the cracking of long-chain LDPE wax into short-chain liquid hydrocarbons (Sriningsih *et al.* 2014). Fig. 4(a) shows the yield of liquid, solid, and gaseous product produced from the hydrocracking of pyrolyzed LDPE plastic. The hydrocracking of pyrolyzed LDPE plastics using Ni-Cu/HZSM-5 catalyst at temperatures of 275 and 300 °C did not produce liquid products. It seemed that the temperatures of 275 to 300 °C were relatively low for the hydrocracking of heavy hydrocarbons such as LDPE. At this temperature, incomplete cracking occurs. The breaking down of long hydrocarbon chains into shorter ones took place, but it seemed not sufficient to produce significant liquid hydrocarbons. Conversely, solid products dominated because heavier solid fractions still exist due to insufficient cracking leading to incondensable solids (Al-Muttaqii *et al.* 2019).

In this study, liquid products were produced from the hydrocracking process at higher temperatures; at temperatures of 325–400 ^{0}C. There was an increase in the amount of liquid products produced at temperatures of 325–375 °C, then a decrease at temperatures of 400 ^{0}C. This increase in the liquid yield at temperatures of 325–375 ^{0}C was due to severe cracking taking place in breaking down long polymer chains into liquid hydrocarbons. The metal sites and acid sites of the catalyst efficiently promoted the cracking reaction at this temperature, increasing the amount of pyrolyzed LDPE converted into liquid products (Al Muttaqii *et al.* 2024). However, the yield of liquid product decreased when higher temperature was employed. At 400 °C, such higher temperatures promoted further cracking to break down liquid hydrocarbons into lighter fractions. Excessive temperatures could also cause catalyst deactivation or changes in selectivity, resulting in more gas than liquid products (Marhaini *et al.* 2024).

The GC-detectable compounds in the liquid product were quantified using a gas chromatograph equipped with a mass spectrometer as the detector. The results were grouped into gasoline (C_5-C_{12}), kerosene (C_{13}-C_{14}), and diesel (C_{15}-C_{20}) fractions. Generally, as the hydrocracking reaction temperature increased, the gasoline fraction produced increased, while the gasoline and diesel fractions decreased (Liu *et al.* 2021). The results of this study showed that the gasoline yield increased in the temperature range of 325-375 ^{0}C from 7.27% to 8.48%. The increase in gasoline yield was caused by the increase in the hydrocracking reaction temperature at 325-375 ^{0}C, which encouraged the breakdown of long polymer chains into short hydrocarbons in the gasoline range (C_5-C_{12}). The highest gasoline product was produced at a temperature of 375 ^{0}C and then decreased at a temperature of 400 ^{0}C with a yield of 6.49%. Further increase in temperature would increase the amount of lighter fraction products such as gas (C_1-C_4), thereby reducing the amount of gasoline product (Wang *et al.* 2023).

The kerosene yield showed an overall downward trend as the hydrocracking reaction temperature increased, from 3.82% at 325 °C to 1.72% at 400 °C. Meanwhile, diesel yield tended to increase with rising temperatures from 8.96% at 325 °C to 11.2% at 375 °C and decreases at 400 °C to 4.07%. As the reaction temperature increased, the yield of kerosene and diesel fractions generally decreases. At high temperatures, the components of the kerosene and diesel fractions will easily crack into fractions with shorter carbon chains, becoming gasoline and gas fractions. This showed that at high temperatures, the components in the liquid product will continue to undergo C–C bond cleavage, resulting in the formation of hydrocarbon fractions with shorter chains (Ma *et al.* 2024).

3.3 Characteristics of Liquid Products Produced from the Hydrocracking of Pyrolyzed LDPE Plastics

The chemical functionalities could greatly affect the chemical properties of the products of hydrocracking of pyrolyzed LDPE. The presence of alkanes, aromatics, and other hydrocarbons contained in the product can provide information about the quality of the product. The chemical functionalities of the liquid product obtained from the hydrocracking of pyrolyzed LDPE using Ni-Cu/HZSM-5 catalyst at various temperatures are shown in Fig. 5. Fig. 5 shows the FTIR results of pyrolysis wax and liquid products from the LDPE plastic hydrocracking process at different temperatures. The IR spectra were taken in the wavelength range of 4000-500 cm^{-1}.

ISSN: 2252-4940/© xxx. The Author(s). Published by CBIORE

Based on the FTIR spectrum obtained, pyrolysis wax and hydrocracking reaction products at various temperatures showed uniform peaks at around 2917, 2850, 1460, 1374, 965, and 722 cm^{-1}, which are characteristic of polyethylene polymers (Yu *et al.* 2022). The peak detected at a wavenumber of 3000-2850 cm^{-1} indicated the presence of C–H bond stretching vibrations (alkanes) in the compound. In this wavenumber range, a new peak was detected at temperatures of 275-400 °C, namely at a wavenumber of 2954 cm^{-1}, but it was not detected in the LDPE wax results. Based on the data produced, the peak intensity appears to increase with the rise in hydrocracking reaction temperature. The presence or increase of this new peak indicated that the alkane hydrocarbon content was greater than that of LDPE wax (Marlinda *et al.* 2017). The absorption bands at wavenumbers 1461 cm^{-1} and 1374 cm^{-1} indicate the presence of $–CH_2$ and $–CH_3$ bending vibrations. At these wavenumbers, it can be seen that as the hydrocracking temperature increases, the peaks become sharper and their intensity increases. This increase in peaks indicates a shortening of the chain during the hydrocracking process and the formation of shorter, more branched hydrocarbons with methyl ($–CH_3$) substituents (Smith 2021). The peak at a wavelength of 965 cm^{-1} indicated the presence of =CH bending vibrations, which indicated the presence of unsaturated hydrocarbons such as alkenes, and the peak at a wavelength of 717-730 cm^{-1} indicated the presence of $–CH_2$ rocking vibrations (Hauli *et al.* 2020).

Several differences between the FTIR results of LDPE wax and the hydrocracking products were observed. A peak at wavenumbers of 3100-3000 cm^{-1} that was assigned as aromatic compounds was observed in pyrolyzed LDPE. This peak was not observed in the liquid products from the catalytic hydrocracking at temperatures of 275-375 °C but was re-observed in those at a temperature of 400 °C. Aromatic compounds in pyrolyzed LDPE would gradually convert into aliphatic or smaller chain of hydrocarbons as the reaction temperature increased. At high temperatures, aromatic compounds can be formed through cyclization and aromatization reactions during the hydrocracking process. The formation of these aromatic compounds would produce hydrocarbon fractions with high octane numbers, so that the product would belong to gasoline fractions (Akhtar *et al.* 2025; Onwudili *et al.* 2009).

A significantly high peak at a wavenumber of 1712 cm^{-1}, which indicated the presence of carbonyl (C=O) bonds was observed in the liquid product from the catalytic hydrocracking at temperatures of 325 and 400 °C. In addition, peaks at wavenumbers of 1300-1000 cm^{-1} that was assigned as the presence of C–O bonds, were observed in all liquid products from the catalytic hydrocracking at all temperatures but not in the pyrolyzed LDPE. This indicated the presence of esters, ethers, carboxylic acids, or aldehydes in the hydrocracking product. These FTIR spectra showed that pyrolyzed LDPE was dominated by saturated alkyls without oxygenation groups. After the hydrocracking process, characteristic peaks such as C=O, C=C, and C–O appear, indicating the formation of compounds such as alkenes, ketones, and esters.

Density values are very important in determining the quality of a fuel oil. Generally, the higher the hydrocracking reaction temperature, the lower the density value will be. Higher temperatures cause long hydrocarbon chains to break down into shorter ones, resulting in lighter hydrocarbon fractions with lower density values (Febriana *et al.* 2020). The density of the liquid products from the catalytic hydrocracking using Ni-Cu/HZSM-5 catalyst is listed in Table 4. The density of the liquid products was measurable for those produced at 325 ^{0}C or higher, as the lower temperatures produced a wax-like products.

The density of the liquid hydrocracking product from 325 °C was 0.80905 g/mL. This value meets the kerosene fuel density standard based on SNI 7390-200, (780-810 kg/m^3). The Directorate General of Oil and Gas of the Republic of Indonesia ruled that the density of diesel and gasoline fuels should be in the range of 815-880 kg/m3 and 715-770 kg/m^3, respectively. It means that the density of the liquid hydrocracking product from temperatures of 350 and 375 °C (0.8210 and 0.8166 g/mL, respectively), has met the standard density for diesel fuel, while those from temperature of 400 ^{0}C (density of 0.7652 g/mL), the density was in suitable with gasoline fractions. These results indicated that the higher the hydrocracking reaction, the lower the density value produced, approaching the density value of gasoline.

Another important property of liquid fuel is the calorific value. The calorific value indicates the amount of heat produced during the combustion of fuel in the presence of oxygen. This heat output is also referred to as the heating value (Darmaningsih *et al.* 2019). The calorific value produced from the hydrocracking of pyrolyzed LDPE in Table 5 showed an insignificant difference of the calorific value for all (wax and) liquid hydrocracking products, ranging from 42-44 MJ/kg. According to *Akhtar et al.* (2025), commercial fuels such as gasoline and diesel have a calorific value of 42-47 MJ/kg, while according to SNI 7182:2012, the calorific value of diesel fuel is between 42-46 MJ/kg. Based on its calorific value, these results indicate that liquid oil products produced from the hydrocracking of LDPE plastic have the potential to be used as an alternative diesel fuel.

6. Conclusion

The results of LDPE plastic conversion through hydrocracking reactions show that increasing the reaction temperature will increase the yield of liquid and gas products, while solid products will decrease. The liquid products of the hydrocracking reaction were analyzed using GC-MS and classified based on hydrocarbon chain length, consisting of gasoline fraction (C_5-C_{12}), kerosene fraction (C_{13}-C_{14}), and diesel fraction (C_{15}-C_{20}). The results of this study show that the gasoline yield increased in the temperature range of 325-375 ^{0}C from 7.27% to 8.48% and decreased at a temperature of 400 ^{0}C. Further temperature increases will increase more products with lighter fractions such as gas (C_1-C_4), thereby reducing the amount of gasoline products. The kerosene and diesel yield results showed an overall downward trend as the hydrocracking reaction temperature increased. FTIR analysis showed that the pyrolysis wax was dominated by saturated alkyls without oxygenation groups. After the hydrocracking process, compounds such as alkenes, ketones, and esters were formed. Increasing the reaction temperature caused further cracking and functionalization reactions, resulting in lighter and more complex products. The higher the hydrocracking reaction temperature, the lower the density value, while the calorific value decreases.

Acknowledgments

The authors would like to thank the National Research and Innovation Agency, the Republic of Indonesia for the research facilities.

ISSN: 2252-4940/© xxx. The Author(s). Published by CBIORE

Author Contributions: S.S.M.: project execution, data analysis, writing—original draft, S.K.; supervision, conceptualization, methodology, formal analysis, writing—review and editing, A.A.D.; supervision, resources, validation, data analysis, E.A.; supervision, data analysis, project administration, validation. All authors have read and agreed to the published version of the manuscript.

Funding: This research was supported by the National Research and Innovation Agency of the Republic of Indonesia for the research facilities.

Conflicts of Interest: The authors declare no conflict of interest.

References

Akça, B., Can, M., Değirmenci, V., Yilmaz, A., & Üner, D. (2007). Single step synthesis of mesoporous Co-Pb/SBA-15 catalysts (K. Eguchi, M. Machida, & I. Yamanaka (eds.); pp. 317–320). *Studies in Surface Science and Catalysis*; https://doi.org/https://doi.org/10.1016/B978-0-444-53202-2.50068-3

Akhtar, M.N., Ahmad, N., & Alqudayri, F. (2025). Catalytic transformation of LDPE into aromatic-rich fuel oil. *Catalysts*, 15(6), 532. https://doi.org/10.3390/catal15060532

Al Muttaqii, M., Marbun, M.P., Sudibyo, S., Aunillah, A., Pranowo, D., Hasanudin, H., Rinaldi, N., & Bardant, T.B. (2024). Conversion of sunan candlenut oil to aromatic hydrocarbons with hydrocracking process over nano-HZSM-5 Catalyst. *Bulletin of Chemical Reaction Engineering and Catalysis*, 19(1), 141–148. https://doi.org/10.9767/bcrec.20116

Al-Muttaqii, M., Kurniawansyah, F., Prajitno, D.H., & Roesyadi, A. (2019). Hydrocracking of coconut oil over Ni-Fe/HZSM-5 catalyst to produce hydrocarbon biofuel. *Indonesian Journal of Chemistry*, 19(2), 319–327; https://doi.org/10.22146/ijc.33590

Al-Salem, S. M., Antelava, A., Constantinou, A., Manos, G., & Dutta, A. (2017). A Review on *Thermal and Catalytic Pyrolysis of Plastic Solid Waste* (PSW). *Journal of Environmental Management*, 197(1408), 177–198; https://doi.org/10.1016/j.jenvman.2017.03.084

Darmaningsih, A., Suwandi, & Fitriyanti, N. (2019). Uji kalor bahan bakar campuran solar dan minyak nabati. *E-Proceeding of Engineering*, 6(1), 1370–1376.

Daryoso, K., Wahyuni, S., & Saputro, H. (2012). Uji aktivitas katalis ni-mo/zeolit pada reaksi hidrorengkah fraksi sampah plastik (polietilen). 1(2252).

Dewan Energi Nasional. (2023). Outlook Energi Indonesia 2023. In Dewan Energi Nasional (2023rd ed.). Dewan Energi Nasional. https://www.esdm.go.id/assets/media/content/content-outlook-energi-indonesia-2019-bahasa-indonesia.pdf

Febriana, I., Ramadhini, T.K., & Aulia, T. (2020). Pengaruh temperatur dan waktu reaksi minyak jelantah dengan zeolit alam pada produksi biofuel. *Jurnal Kinetika*, 11(3), 53–59.

Genet, M.B., Sendekie, Z.B., & Jembere, A.L. (2021). Investigation and optimization of waste LDPE plastic as a modifier of asphalt mix for highway asphalt: case of Ethiopian roads. *Case Studies in Chemical and Environmental Engineering*, 4, 100150; https://doi.org/10.1016/j.cscee.2021.100150

Gorzin, F., Towfighi Darian, J., Yaripour, F., & Mousavi, S.M. (2018). Preparation of hierarchical HZSM-5 zeolites with combined desilication with $NaAlO_2$/tetrapropylammonium hydroxide and acid modification for converting methanol to propylene. *RSC Advances*, 8(72), 41131–41142; https://doi.org/10.1039/c8ra08624a

Hariadi, D., Saleh, S.M., Anwar Yamin, R., & Aprilia, S. (2021). Utilization of LDPE plastic waste on the quality of pyrolysis oil as an asphalt solvent alternative. *Thermal Science and Engineering Progress*, 23, 100872; https://doi.org/10.1016/j.tsep.2021.100872

Hauli, L., Wijaya, K., & Syoufian, A. (2020). Fuel production from LDPE-based plastic waste over chromium supported on sulfated zirconia. *Indonesian Journal of Chemistry*, 20(2), 422–429; https://doi.org/10.22146/ijc.45694

Karim, T.M., Toyoda, H., Sawada, M., Zhao, L., Wang, Y., Xiao, P., Wang, L., Huang, J., & Yokoi, T. (2024). Aluminum distribution on the microporous and hierarchical ZSM-5 intracrystalline and its impact on the catalytic performance. *Chem & Bio Engineering,* 1(9), 805-816; https://doi.org/10.1021/cbe.4c00117

Khromova, S.A., Smirnov, A.A., Bulavchenko, O.A., Saraev, A.A., Kaichev, V.V, Reshetnikov, S.I., & Yakovlev, V.A. (2014). Applied catalysis A : General anisole hydrodeoxygenation over Ni–Cu bimetallic catalysts: The effect of Ni/Cu ratio on selectivity. *Applied Catalysis A: General*, 470, 261–270. https://doi.org/10.1016/j.apcata.2013.10.046

Lao, K., Liu, X., Lin, H., Wen, L., Pan, Y., Hu, T., Tao, H.B. & Zheng, N. (2025). Is high specific surface area essential for anode catalyst supports in proton exchange membrane water electrolysis? *Materials Horizons*, 12(21), 9069-9078; https://doi.org/10.1039/D5MH01127B

Li, L., Zuo, J., Duan, X., Wang, S., & Chang, R. (2022). Converting waste plastics into construction applications: A business perspective. *Environmental Impact Assessment Review*, 96(January), 106814; https://doi.org/10.1016/j.eiar.2022.106814

Liu, S., Kots, P.A., Vance, B.C., Danielson, A., & Vlachos, D.G. (2021). Plastic waste to fuels by hydrocracking at mild conditions. *Science Advances*, 7(17), 1–10; https://doi.org/10.1126/sciadv.abf8283

Ma, W., Wang, C., Chen, Z., Yan, S., Cao, S., Wang, X., Chen, Y., Yang, H., & Chen, H. (2024). Catalytic hydrogenolysis of polypropylene and polyethylene mixtures: Effect of temperature on liquid alkane components. *Journal of the Energy Institute*, 115(January), 101615; https://doi.org/10.1016/j.joei.2024.101615

Marbun, A.P., Ainin, Emawati NKD, A., Nabila, D., Samara, G. A., Sani, M. A., Negari, N., Deviani, N., Woro W, S. A., Setiawan, S., Fauhan, Z. A., & Erwandi, D. (2021). Upaya penggantian sampah plastik dalam pengemasan komoditi online shop oleh pelaku UMKM. *Jurnal Pengabdian Kesehatan Masyarakat*, 1(2), 145–152.

Marhaini, M., Fernianti, D., & Aulia, M.R. (2024). Effective pyrolysis of LDPE plastic waste to fuel using titanium dioxide catalyst. *International Journal of Advanced and Applied Sciences*, 11(12), 75–82; https://doi.org/10.21833/ijaas.2024.12.009

Marlinda, L., Al-Muttaqii, M., Gunardi, I., Roesyadi, A., & Prajitno, D.H. (2017). Hydrocracking of Cerbera manghas oil with Co-Ni/HZSM-5 as double promoted catalyst. *Bulletin of Chemical Reaction Engineering & Catalysis*, 12(2), 167–184; https://doi.org/10.9767/bcrec.12.2.496.167-184

Munir, D., Irfan, M.F., & Usman, M. R. (2018). Hydrocracking of virgin and waste plastics: A detailed review. *Renewable and Sustainable Energy Reviews*, 90(June 2016), 490–515; https://doi.org/10.1016/j.rser.2018.03.034

Nugrahaningtyas, K.D., Sabiilagusti, A. I., Rahmawati, F., Heraldy, E., & Hidayat, Y. (2024). Hydrodeoxygenation of anisole via Cu supported on zeolite: HZSM-5, MOR, and Indonesian activated natural zeolite. *Chemical, Food, and Environmental Engineering*, 44(1). e106683 1-10; https://doi.org/10.15446/ing.investig.106683

Onwudili, J.A., Insura, N., & Williams, P.T. (2009). Composition of products from the pyrolysis of polyethylene and polystyrene in a closed batch reactor: Effects of temperature and residence time. *Journal of Analytical and Applied Pyrolysis*, 86(2), 293–303; https://doi.org/10.1016/j.jaap.2009.07.008

Qin, L., Li, J., Zhang, S., Liu, Z., Li, S., & Luo, L. (2023). Catalytic performance of Ni-Co/HZSM-5 catalysts for aromatic compound promotion in simulated bio-oil upgrading. *RSC Advances*, 13(11), 7694–7702; https://doi.org/10.1039/d2ra07706j

Savitri, S., Nugraha, A.S., & Aziz, I. (2016). Pembuatan katalis asam ($Ni/\gamma\text{-}Al_2O_3$) dan katalis basa ($Mg/\gamma\text{-}Al_2O_3$) untuk aplikasi pembuatan biodiesel dari bahan baku minyak jelantah. *Jurnal Kimia Valensi*, 2(1), 1–10.

Sinaga, S.V., Haryanto, A., & Triyono, S. (2014). Pengaruh suhu dan waktu reaksi pada pembuatan biodiesel dari minyak jelantah [Effects of temperature and reaction time on the biodiesel production using waste cooking oil]. *Jurnal Teknik Pertanian Lampung*, 3(1), 27–34.

Smith, B. C. (2021). The infrared spectra of polymers II: Polyethylene. spectroscopy, 36(9), 24-29; https://doi.org/https://doi.org/10.56530/spectroscopy.xp7081p7

Sriningsih, W., Saerodji, M. G., Trisunaryanti, W., Triyono, Armunanto, R., & Falah, I.I. (2014). Fuel production from LDPE plastic waste over natural zeolite supported Ni, Ni-Mo, Co and Co-Mo metals.

Procedia Environmental Sciences, 20, 215–224; https://doi.org/10.1016/j.proenv.2014.03.028

Surono, U. (2013). Berbagai metode konversi sampah plastik menjadi bahan bakar minyak. *Jurnal Teknik*, 3(1), 32–40.

Tursunov, O., Kustov, L., & Tilyabaev, Z. (2019). Catalytic activity of H-ZSM-5 and Cu-HZSM-5 zeolites of medium SiO_2/Al_2O_3 ratio in conversion of n-hexane to aromatics, *Journal of Petroleum Science and Engineering*, 180, 773-778; https://doi.org/10.1016/j.petrol.2019.06.013

Valizadeh, S., Jang, S.H., Rhee, G.H., Lee, J., Show, P.L., Khan, M.A., Jeon, B.H., Lin, K.Y.A., Ko, C.H., Chen, W.H., & Park, Y.K. (2022). Biohydrogen production from furniture waste via catalytic gasification in air over Ni-loaded ultra-stable Y-type zeolite. *Chemical Engineering Journal*, 433(P3), 133793; https://doi.org/10.1016/j.cej.2021.133793

Wang, H., Yoskamtorn, T., Zheng, J., Ho, P.L., Ng, B., & Tsang, S.C.E. (2023). Ce-promoted Pt Sn-based catalyst for hydrocracking of polyolefin plastic waste into high yield of gasoline-range products. *ACS Catalysis*, 13(24), 15886–15898; https://doi.org/10.1021/acscatal.3c03996

Wang, W., Zhang, C., Chen, G., & Zhang, R. (2019). Influence of CeO_2 addition to Ni-Cu/HZSM-5 catalysts on hydrodeoxygenation of bio-oil. *Applied Sciences (Switzerland)*, 9(6), 1257; https://doi.org/10.3390/app9061257

Wardhana, P.B.W., Hanafi, A.F., Finali, A., & Umar, M.L. (2022). Potensi limbah plastik sebagai sumber energi terbarukan menggunakan proses degradasi termal dan katalitik. *J-Proteksion: Jurnal Kajian Ilmiah dan Teknologi Teknik Mesin*, 7(1), 14–20; https://doi.org/10.32528/jp.v7i1.8242

Yu, F., Wu, Z., Wang, J., Li, Y., Chu, R., Pei, Y., & Ma, J. (2022). Effect of landfill age on the physical and chemical characteristics of waste plastics / microplastics in a waste landfill sites. *Environmental Pollution*, 306(February), 119366; https://doi.org/10.1016/j.envpol.2022.119366

Zheng, Y., Wang, J., Li, D., Liu, C., Lu, Y., Lin, X., & Zheng, Z. (2021). Activity and selectivity of Ni–Cu bimetallic zeolites catalysts on biomass conversion for bio-aromatic and bio-phenols. *Journal of the Energy Institute*, 97, 58–72; https://doi.org/10.1016/j.joei.2021.04.008

Zou, J., Fan, C., Jiang, Y., Liu, X., Zhou, W., Xu, H., & Huang, L. (2021). A preliminary study on assessing the brunauer-emmett-teller analysis for disordered carbonaceous materials. *Microporous and Mesoporous Materials,* 327(June), 111411; https://doi.org/10.1016/j.micromeso.2021.111411

Zultiniar, Yelmida, A., & Shiqhi, N. (2017). Impregnasi Logam Cu Pada Hidroksiapatit dari Kulit Kerang Darah (Anadara granosa). *Jurnal Sains dan Teknologi*, 16(1), 20–23.

List of Table

Table 1. Elemental composition of HZSM-5 and Ni-Cu/HZSM-5

Table 2. Elemental composition of HZSM-5 and Ni-Cu/HZSM-5 measured using EDX spectroscopy

Table 3. Results of BET-BJH and NH3-TPD analysis of HZSM-5 and Ni-Cu/HZSM-5.

Table 4. The density and calorific values of the liquid hydrocracking products using a Ni-Zu/HZSM-5 catalyst at temperatures of 275-400 °C.

Table 1
Elemental composition of HZSM-5 and Ni-Cu/HZSM-5

Element	Composition (wt%)	
	HZSM-5	Ni-Cu/HZSM-5
Si	43.00	39.40
Cu	-	3.10
Al	2.90	2.80
Ni	-	2.80
Mg	0.90	0.80
P	0.20	0.20
Ca	0.10	0.20
S	0.10	0.20
Fe	0.10	0.10
Trace	0.20	0.10

Table 2
Elemental composition of HZSM-5 and Ni-Cu/HZSM-5 measured using EDX spectroscopy

Sample	Elemental Composition (%)				
	Si	O	Al	Ni	Cu
HZSM-5	42.6	55.1	2.3	-	-
Ni-Cu/HZSM-5	36.4	45.0	2.0	2.7	13.9

Table 3
Results of BET-BJH and NH_3-TPD analysis of HZSM-5 and Ni-Cu/HZSM-5.

Sample	Surface Area (m^2/g)	Pore Diameter (nm)	Pore Volume (cm^3/g)	Acidity (mmol/g)
HZSM-5	201.699	1.9119	0.1537	3.2679
Ni-Cu/HZSM-5	271.167	1.9125	0.2040	2.4631

Table 4
The density and calorific values of the liquid hydrocracking products using a Ni-Zu/HZSM-5 catalyst at temperatures of 275-400 °C.

Temperature (°C)	Density (g/mL)	Calorific Value (MJ/kg)
275	-	43.9277
300	-	43.5174
325	0.80905	44.1614
350	0.8210	44.3124
375	0.8166	42.6437
400	0.7652	44.6004

ISSN: 2252-4940/© xxx. The Author(s). Published by CBIORE

List of Figure

Figure 1. The diffraction patterns of (a) HZSM-5 and (b) Ni-Cu/HZSM-5 with 5% total metal loading and Ni:Cu ratio of 1:1.
Figure 2. Surface morphology of (a) HZSM-5 and (b) Ni-Cu/HZSM-5 at 10,000x magnification and elemental mapping results of (c) Ni-Cu/HZSM-5, dispersion of (d) Ni and (e) Cu elements
Figure 3. Adsorption-desorption isotherm of liquid nitrogen at the HZSM-5 and Ni-Cu/HZSM-5 surface.
Figure 4. (a) Yield of liquid, solid, and gaseous products and (b) yield of fuel fractions in liquid products produced during the hydrocracking of pyrolyzed LDPE using Ni-Cu/HZSM-5 catalyst.
Figure 5. FTIR spectra of (a) pyrolyzed LDPE and the liquid products obtained from the hydrocracking of pyrolyzed LDPE at (b) 275 °C, (c) 300 °C, (d) 325 °C, (e) 350 °C, (f) 375 °C, and (g) 400 °C using Ni-Cu/HZSM-5 catalyst.

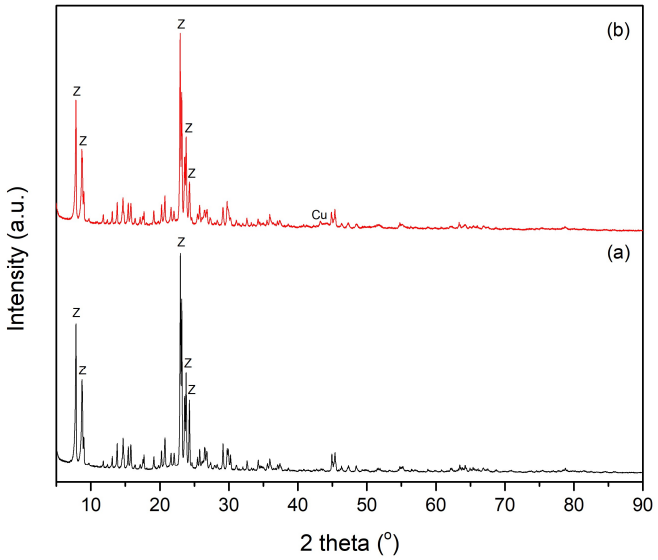

Fig. 1 The diffraction patterns of (a) HZSM-5 and (b) Ni-Cu/HZSM-5 with 5% total metal loading and Ni:Cu ratio of 1:1.

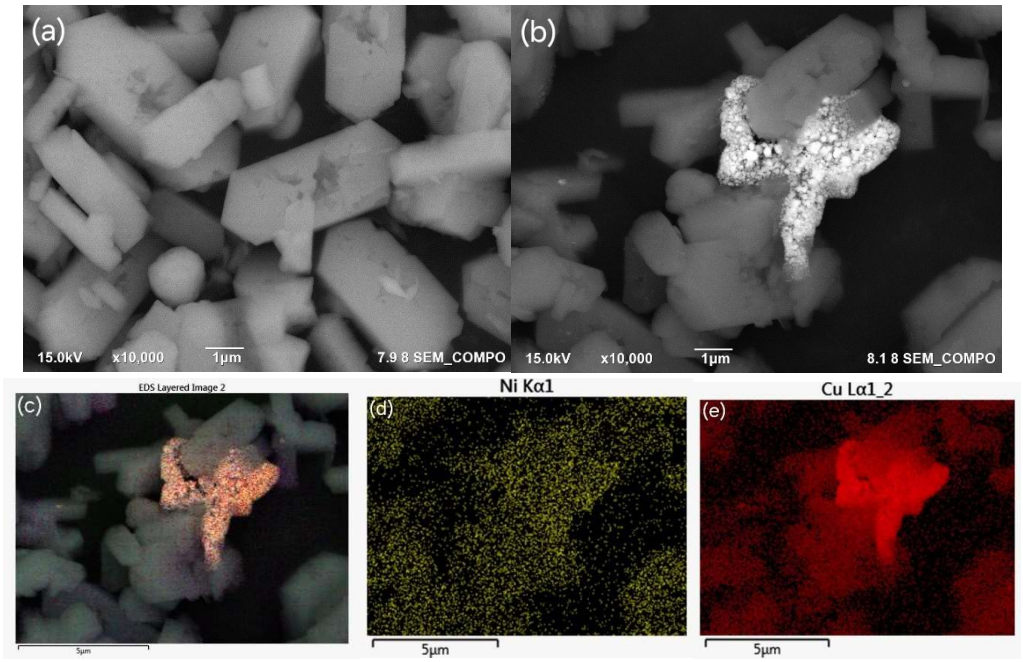

Fig. 2 Surface morphology of (a) HZSM-5 and (b) Ni-Cu/HZSM-5 at 10,000x magnification and elemental mapping results of (c) Ni-Cu/HZSM-5, dispersion of (d) Ni and (e) Cu elements

ISSN: 2252-4940/© xxx. The Author(s). Published by CBIORE

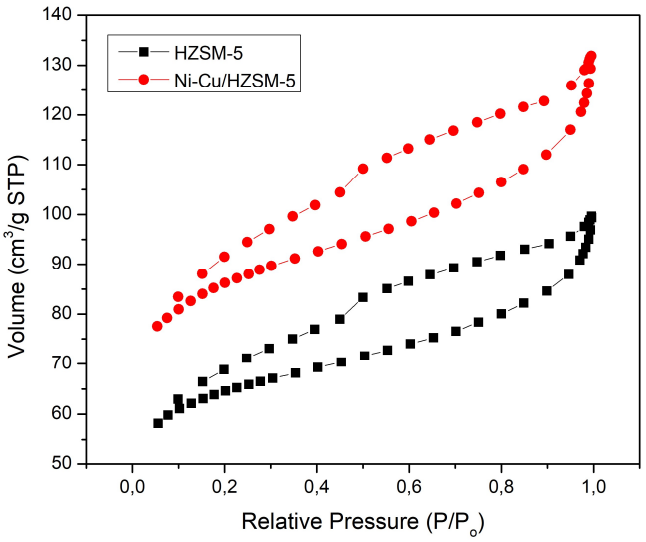

Fig. 3 Adsorption-desorption isotherm of liquid nitrogen at the HZSM-5 and Ni-Cu/HZSM-5 surface.

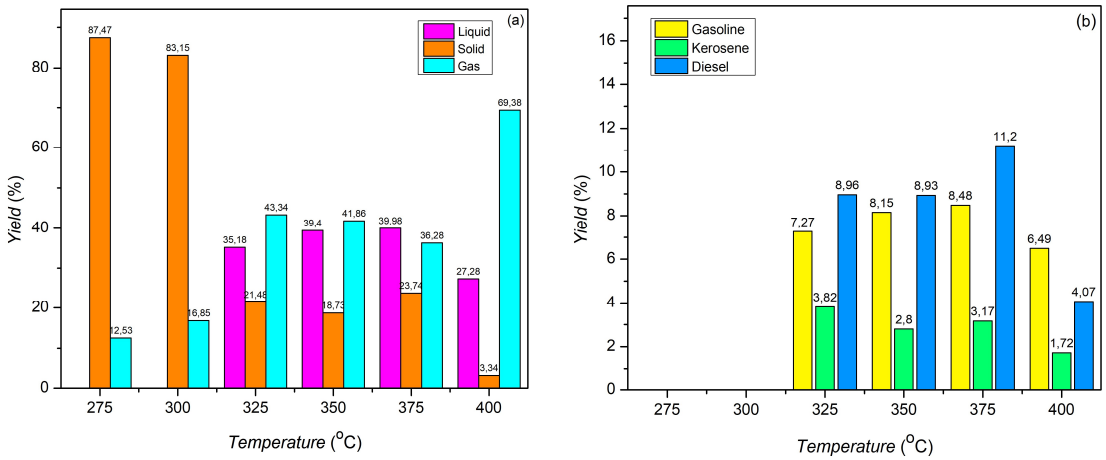

Fig. 4 (a) Yield of liquid, solid, and gaseous products and (b) yield of fuel fractions in liquid products produced during the hydrocracking of pyrolyzed LDPE using Ni-Cu/HZSM-5 catalyst.

ISSN: 2252-4940/© xxx. The Author(s). Published by CBIORE

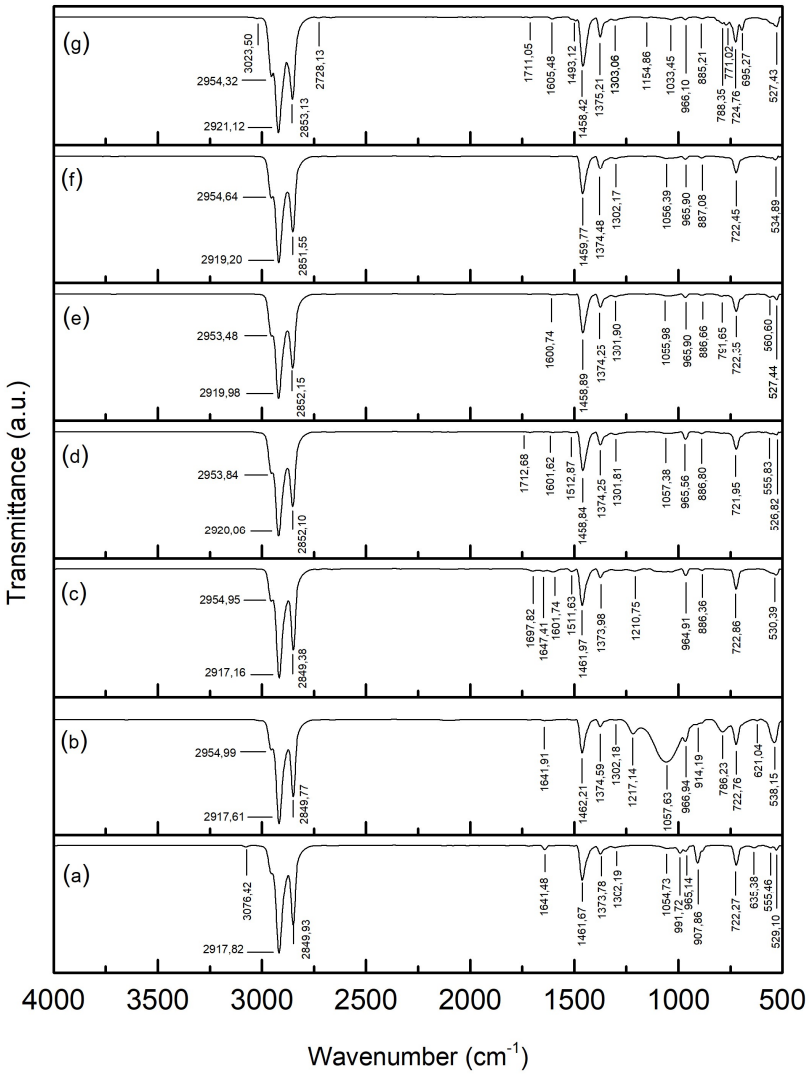

Fig. 5 FTIR spectra of (a) pyrolyzed LDPE and the liquid products obtained from the hydrocracking of pyrolyzed LDPE at (b) 275 °C, (c) 300 °C, (d) 325 °C, (e) 350 °C, (f) 375 °C, and (g) 400 °C using Ni-Cu/HZSM-5 catalyst.

ISSN: 2252-4940/© xxx. The Author(s). Published by CBIORE